JOURNAL OF COMPUTATIONAL PHYSICS 19, 150–178 (1975)

Three-Dimensional Supersonic Flow of a Viscous or Inviscid Gas

H. McDONALD AND W. R. BRILEY

United Technologies Research Center, East Hartford, Connecticut 06108

Received February 14, 1975

The initial-boundary value problem representing the supersonic flow of a viscous or inviscid gas is solved by a forward marching procedure which integrates a set of coupled nonlinear multidimensional equations. The numerical method is based upon an alternating-direction implicit scheme and sample calculations have been performed to demonstrate the capabilities of the procedure. The specific problem considered concerns the supersonic flow of a three-dimensional jet exhausting into a supersonic ambient stream. It is shown that stable and apparently accurate solutions can be obtained for axial steps considerably larger than those normally permissible with many conditionally stable procedures. The computational cost per grid point per axial step in the present problem was very approximately only a factor of 2 greater than that required with the conditionally stable methods.

INTRODUCTION

A viscous compressible fluid in the continuum flow regime satisfies the Navier–Stokes equations. The term "viscous" is herein applied in a generic sense in that flows wherein significant transport occurs by virtue of the turbulent Reynolds stresses are also considered to be "viscous." This latter practice stems from the widespread use of an effective viscosity to introduce the turbulent stresses into the equations of mean motion. Examples of supersonic viscous flows are to be found in the flow around and behind bodies traveling at supersonic speeds within the atmosphere and in such exotic devices as continuous wave chemical lasers.

If the flow is assumed to be inviscid the Navier–Stokes equations reduce to the Euler equations, and if, further, the flow is everywhere supersonic, the governing equations are hyperbolic and proved numerical schemes are available and have been applied to predict the flow field arising from very complex body shapes. However, the viscosity, although small, can be of considerable practical concern; for instance, in determining heat transfer rates to the body surface. The usual method of allowing for viscous effects is to assume the flow is primarily unidirectional and the layer where viscosity can affect the mean flow is thin so that transverse gradients are much greater than axial gradients, and that the pressure within the viscous

layer is that impressed by the adjacent inviscid stream. By means of these assumptions the Navier–Stokes equations may be reduced to the much more tractable boundary layer equations which form an intitial-boundary value problem. The thin boundary-layer or shear layer concept has proved very valuable in fluid mechanics but in certain circumstances cannot be applied, for instance in a supersonic underexpanded jet mixing problem, since initially mixing occurs along the jet boundaries but eventually extends down to the jet centerline and complex pressure changes occur within the mixing region. The three-dimensional boundary layer equations are normally thought of as containing a diffusive flux in only one coordinate direction; that is, both axial and spanwise diffusive effects are negligible. Recently, however, considerable attention has been devoted to three-dimensional viscous flows where only the axial diffusive flux is neglected. The resulting procedures have shown considerable promise for treating such important practical problems as, for instance, the boundary layer corner flow and the viscous flow within ducts of arbitrary cross section. The present work stems from an interest in developing a very efficient numerical procedure for treating three-dimensional viscous flows at high Reynolds numbers where it is reasonable to neglect axial diffusive fluxes.

Insofar as previous work on this area is concerned, Caretto, Curr, and Spalding [1] have devised an implicit method which employs iterative point relaxation to solve the coupled nonlinear system derived from the Navier–Stokes equations with axial diffusion neglected. Caretto *et al.* were concerned with steady three-dimensional subsonic duct flow and uncoupled the axial pressure gradient from the cross-sectionally varying contribution. Since point relaxation generally converges slowly, it was felt that a considerable improvement in efficiency, particularly with dense meshes, could be achieved by use of a more efficient algorithm. Dense meshes are, of course, frequently required in practical problems. Patankar and Spalding [2] further developed the procedure of Caretto *et al.* by developing a line relaxation procedure which solves an uncoupled linearized difference system. In spite of the resulting improvement in efficiency, the uncoupling of the equations and the linearization leave open to question the capability of the Patankar–Spalding procedure to allow for strong coupling between equations and the method's ability to take large streamwise steps while retaining accuracy. In an effort to develop a high-efficiency method of treating the same reduced Navier–Stokes equations, Briley [3] applied an alternating-direction implicit (ADI) technique to an uncoupled linearized system iteratively. Subsequent experience with this technique, particularly with regard to the effect of compressibility, led to the development of the present procedure.

All the procedures referred to above were developed primarily for treating subsonic or incompressible flows. Nardo and Cresci [4], however, treated a very similar set of governing equations in considering the boundary layer on a finite

plate at hypersonic speeds. The numerical method developed by Nardo and Cresci applied an ADI technique to a coupled but linearized system. The pressure was assumed constant in the axial (marching) direction and the band matrix arising from the application of the ADI technique was solved by Gaussian elimination. More recently, Rubin and Lin [5] considered the hypersonic leading edge problem and treated almost the same equations as Nardo and Cresci with the exception that in this instance all the pressure terms were retained. To solve their equations Rubin and Lin developed an efficient numerical method for initial-boundary value problems which treats the coupled nonlinear system by means of a semi-implicit predictor–corrector iterative scheme. Using this technique, Rubin and Lin were able to demonstrate clearly the very considerable gains in efficiency possible, vis-à-vis explicit procedures suffering from a viscous stability limitation, for treating this type of problem. In view of the Rubin–Lin findings, explicit techniques are not considered further in this study. In their work Rubin and Lin also considered an ADI procedure as a candidate method of solving their particular problem. However, difficulty in obtaining stable solutions with large axial steps caused Rubin and Lin to abandon their ADI scheme in favor of the predictor–corrector scheme mentioned above. Several points should be noted at this juncture, however. First, no details concerning the precise ADI scheme considered by Rubin and Lin are available. In particular, it is not known how the linearization was carried out or how any nonlinear updating, if done, was implemented and both of these factors can have a major effect on the solution. Second, by using a predictor–corrector technique a penalty is incurred vis-à-vis a noniterative ADI scheme if more than one corrector step is used and Rubin and Lin routinely used three corrector steps. Thus, there remain gains in efficiency to be had if a stable accurate ADI scheme can be made to work taking large axial steps. In view of the authors' previous favorable experience with ADI methods, the present study was embarked upon.

For the present, attention is restricted to flows that are everywhere supersonic, since in this instance the governing equations can be solved as an initial-boundary value problem without any assumptions about the pressure field. For subsonic flow, however, the inviscid flow region is known to be governed by elliptic equations, and in this circumstance, some means for satisfying downstream boundary conditions is required. One method for circumventing this problem for subsonic flows is to assume that the pressure field appropriate for irrotational inviscid flow in the geometry of interest represents a given, reasonable first approximation to the actual pressure field. Thus, inviscid axial pressure gradients can be imposed upon the flow, much as in conventional boundary layer theory. Some preliminary results for subsonic flow in curved passages following this approach and using essentially the present numerical techniques have recently been computed by Briley and McDonald [6]. In addition, only the principal terms in the stress

tensor are included in the work discussed here and a temperature-independent viscosity has been assumed, although these restrictions have been removed in work now underway.

Governing Equations

The Navier–Stokes equations governing the steady flow of a viscous gas can be written in Cartesian coordinates as

$$\frac{\partial}{\partial x}\left(\rho u\tilde{u} - \mathrm{R_e}^{-1}\frac{\partial \tilde{u}}{\partial x}\right) + \frac{\partial}{\partial y}\left(\rho v u - \mathrm{R_e}^{-1}\frac{\partial \tilde{u}}{\partial y}\right) + \frac{\partial}{\partial z}\left(\rho\omega\tilde{u} - \mathrm{R_e}^{-1}\frac{\partial \tilde{u}}{\partial z}\right)$$

$$= \frac{\partial}{\partial \tilde{x}}(-p + \nabla \cdot u/3\mathrm{R_e}), \tag{1}$$

where $\tilde{u}$, $\tilde{x} = u, x; v, y; \omega, z$, respectively, for the x, y, and z momentum equations. The continuity equation is written

$$\frac{\partial}{\partial x}(\rho u) + \frac{\partial}{\partial y}(\rho v) + \frac{\partial}{\partial z}(\rho\omega) = 0. \tag{2}$$

In the above, u, v, and ω are the components of the velocity vector $\bar{u}$ in the x, y, and z directions, ρ is the density, and the variables have normalized appropriately with reference quantities u_r, ρ_r, and all lengths normalized by L_r. The pressure p is normalized by the reference dynamic head $\rho_r u_r^2$ and the Reynolds number Re is defined as $\rho_r u_r L_r/\mu$, where μ is the usual coefficient of viscosity. ∇ is the usual gradient operator.

In the manner outlined in [1–5], a set of approximate equations may be derived from the Navier–Stokes equations by neglecting viscous diffusion in the primary flow direction. If attention is restricted to flows which are everywhere supersonic in this primary flow direction, the set of approximate equations may be solved by a forward marching technique without further simplification. To illustrate the numerical technique without undue complication while retaining the essential features of the problem, a temperature independent viscosity is assumed and only that portion of the stress tensor which appears in incompressible flow is retained. A constant stagnation temperature is also assumed. The resulting system is free from mixed derivatives and although mixed derivatives are permissible within the ADI framework, their formal treatment is somewhat time consuming. Prior experience with a very similar numerical procedure applied to the Navier–Stokes equations [7] has indicated that in viscous flow problems with a predominant primary flow such mixed derivatives can be quite satisfactorily lagged across a

streamwise marching step. With these approximations the Navier–Stokes equations become, with x the primary flow direction,

$$\frac{\partial}{\partial x}(\rho u\tilde{u}) + \frac{\partial}{\partial y}(\rho v\tilde{u}) + \frac{\partial}{\partial z}(\rho\omega\tilde{u}) = -\frac{\partial p}{\partial \tilde{x}} + \mathrm{Re}^{-1}\left(\frac{\partial^2\tilde{u}}{\partial y^2} + \frac{\partial^2\tilde{u}}{\partial z^2}\right), \quad (3)$$

where $\tilde{u}$, $\tilde{x} = u, x; v, y; \omega, z$. The continuity equation is unchanged and the perfect gas law, together with the equation of state, serves to relate pressure to density and velocity; that is,

$$p = A\rho + B\rho(u^2 + v^2 + \omega^2), \quad (4)$$

$$A = RT^0/u_r^2, \quad (5)$$

$$B = -R/2Cp, \quad (6)$$

where R is the gas constant, C_p is the specific heat at constant pressure, and T^0 is the constant stagnation temperature. Thus, the pressure can be eliminated from the momentum equations and the resulting set, together with continuity equation, forms a coupled system of nonlinear equations which is solved numerically. No particular additional problem is posed by allowing the stagnation temperature to vary as this simply requires an energy equation to form part of the system. It can also be shown that the system of governing equations may be reinterpreted as the two-dimensional compressible time-dependent Navier–Stokes equations, in the present case, with a simplified stress tensor. The analogy only requires the streamwise direction to be reinterpreted as a time coordinate with minor changes (simplifications) to the variables within the marching derivatives. For this reason the present scheme could perform a time-dependent Navier–Stokes calculation with some very small changes to the computer code and frequently in the present note the marching direction is referred to as the time or pseudotime coordinate.

Numerical Method

The approximate governing equations form an initial boundary value problem but are nonlinear, coupled, and at any streamwise station pose a two-dimensional problem in the cross-sectional plane. These three aspects of the overall problem are treated in turn. For convenience, a shorthand difference notation is introduced where, if ϕ is any variable located at the i, j grid point in the y, z direction of the cross-sectional plane, then, for instance, with equally spaced points and central differences, difference operators δ_y and $\delta_y{}^2$ are introduced such that

$$\delta_y\phi^n = (\phi^n_{i+1} - \phi^n_{i-1})/2\Delta y = \frac{\partial\phi}{\partial y}\Big|^n_{i,j} + O(\Delta y^2), \quad (7)$$

$$\delta_y{}^2\phi^n = (\phi^n_{i+1} - 2\phi_i{}^n + \phi^n_{i-1})/(\Delta y)^2 = \frac{\partial^2\phi}{\partial y^2}\Big|^n_{i,j} + O(\Delta y^2), \quad (8)$$

with similar definitions of δ_z and $\delta_z{}^2$. It is assumed that the solution is known at cross-sectional plane n and it is desired to march to plane $n + 1$. The Δ symbol denotes the usual difference relationship, $\Delta y = y_{j+1} - y_i$.

The Linearization Process

A major factor in the successful utilization of implicit techniques is the quality of the linear difference approximations to the nonlinear differential equations. It should be pointed out that even when applied to nonlinear systems all implicit schemes now available eventually reduce to the solution of a system of linear equations. It is clear that the capability of stable implicit methods to take large axial steps is of no consequence if the linear difference approximation is a poor representation of the nonlinear system and, consequently, either a small axial step or a large number of iterations will be required to preserve accuracy. A number of previous methods of treating a nonlinear system implicitly are discussed by Ames [8, p. 82] and von Rosenberg [9, p. 56]. Of particular note are the methods based on the generalized Newton–Raphson technique where differencing is used to obtain nonlinear algebraic equations which are then solved iteratively as a sequence of systems of linear equations. Although an attractive technique, it can readily be determined that the computational effort involved in one Newton–Raphson iteration is commensurate with the effort required to march one axial step. The question then arises as to whether or not the same accuracy could be achieved for a given computational effort by taking fewer Newton–Raphson iterations and reducing the axial marching step. The question of accuracy also brings up the point that it is not efficient to reduce the errors arising from the nonlinearity below the truncation error arising from the basic differencing unless some other feature of the method, such as stability, is enhanced. A number of other linearization techniques have been proposed and some have fallen into a predictor–corrector category. As with the Newton–Raphson approach, care must be taken to ensure both convergence and a gain in computational efficiency relative to simply reducing the axial step.

In a companion study Briley and McDonald [7] applied a noniterative linearization technique in developing an implicit procedure for solving the multidimensional compressible Navier–Stokes equations. The linearization was based on a Taylor expansion of the nonlinear terms about the known level solution. In order to illustrate this technique and introduce the concepts of the relationship of truncation error arising from linearization to truncation errors arising from spatial discretization, consider the nonlinear ordinary differential equation

$$d\phi/dx = f(\phi), \tag{9}$$

with exact solution $\phi = \Phi(x)$. Using the mean value theorem a centered difference between levels $n + 1$ and n leads to

$$(\phi^{n+1} - \phi^n)/\Delta x = \tfrac{1}{2}(f^{n+1} + f^n) - (\Delta x^2/12)\,\Phi'''(x_i), \tag{10}$$

where $x_n < x_i < x_{n+1}$. The central problem now is to obtain a satisfactory representation of f^{n+1} which contains only linear contributions from ϕ^{n+1}. This is done by expanding about the n level as follows,

$$f^{n+1} = f^n + \left(\frac{df}{d\phi}\right)^n \Delta\phi + \left(\frac{d^2f}{d\phi^2}\right)^n \cdot \frac{\Delta\phi^2}{2} + O(\Delta\phi^3), \tag{11}$$

and again by expansion about the n level,

$$\phi^{n+1} = \phi^n + \Delta x \left(\frac{d\phi}{dx}\right)^n + \frac{\Delta x^2}{2}\left(\frac{d^2\phi}{dx^2}\right)^n + O(\Delta x^3). \tag{12}$$

Thus from Eq. (12), the error in Eq. (10) arising from retaining only linear terms in the representation of f^{n+1} given by Eq. (11), termed the nonlinear truncation error (NLTE), is of the order

$$\frac{1}{4}\left(\frac{d^2f}{d\phi^2}\right)^n \left[\Delta x \left(\frac{d\phi}{dx}\right)^n + \frac{\Delta x^2}{2}\left(\frac{d^2\phi}{dx^2}\right)^n\right]^2$$

$$= \frac{1}{4}\left(\frac{d}{dx}\left\{\frac{df}{dx}\Big/\frac{d\phi}{dx}\right\}\Big/\frac{d\phi}{dx}\right)^n \left[\Delta x^2 \left(\frac{d\phi^2}{dx}\right)^n + \cdots + O(\Delta x^3)\right] \tag{13}$$

$$\approx \frac{1}{4}\Delta x^2\,[\Phi'''(x_i) - \Phi''^2(x_i)/\Phi'(x_i)], \qquad \text{where } f = \Phi'(x_i) \neq 0, \tag{14}$$

whereas the spatial truncation error (STE) in Eq. (10) is of order $(\Delta x^2/12)\,\Phi'''(x_i)$. Both truncation errors are of the same formal order so that in this example it is obviously inappropriate in general to proceed to improve only the NLTE by, say, a Newton–Raphson technique or a predictor–corrector procedure, since the effort involved is more effectively expended by decreasing the step size Δx which would, consequently, decrease both the NLTE and the STE.

On the basis of the results of the simple example shown above, several additional points are suggested, notably that possibly certain ad hoc linearizations could effectively reduce the order of the truncation error of the overall method. Furthermore, an optimum situation is where the NLTE and the STE are of the same order. Since the overall truncation error is determined by the lowest-order error, the effort required to obtain the higher-order truncation error, be it NLTE or STE, must be carefully weighed against the lack of improvement in the overall method truncation

error. Should a case arise where the NLTE is the determining factor, this error can be reduced in the present linearization by taking additional terms into account in the expansion about the known time level. These additional terms may be evaluated in a number of different ways, by iteration across a step, for instance, but once again care must be taken to ensure that the result is worth the effort. In this regard, the degree of iteration consistent with the spatial truncation error in the present linearization is quite evident, unlike, for instance, some of the techniques for solving the nonlinear difference equations where careful establishment of the convergence criterion (or number of allowable iterations) is necessary.

The procedure may be formalized for a typical system with ϕ a function of x, y,

$$\frac{\partial}{\partial x} H(\phi) = F(\phi) \frac{\partial}{\partial y} G(\phi). \tag{15}$$

Centering between the $n + 1$ and n levels and proceeding as in Eqs. (9)–(12) yields

$$\frac{H(\phi_i^{n+1}) - H(\phi_i^n)}{\Delta x} = F(\phi_i^n)\, \delta_y G(\phi_i^n) + \frac{1}{2} \Big\{ F(\phi_i^n)\, \delta_y \Big[\Big(\frac{dG(\phi)}{d\phi} \Big)_i^n (\phi_i^{n+1} - \phi_i^n) \Big] + \Big(\frac{dF(\phi)}{d\phi} \Big)_i^n (\phi_i^{n+1} - \phi_i^n)\, \delta_y G(\phi_i^n) \Big\} + O(\Delta x^2, \Delta y^2). \tag{16}$$

If $H(\phi)$ were simply equal to ϕ, the expansion given by Eq. (16) is both linear and second order, and could then be utilized in the implicit elimination without further manipulation. If, further, $F(\phi)$ were unity and $G(\phi)$ were equal to ϕ, the conventional Crank–Nicolson scheme is recovered. It is worth observing at this point that Briley and McDonald [7] developed a first-order-accurate linearization requiring only two levels of storage. However, in [7], one of the primary objectives was computing a steady solution as the asymptotic limit of an unsteady calculation, and since temporal accuracy was not overly important for this objective, a first-order-accurate procedure was sufficient. In the present application, however, second-order accuracy for the pseudotime or marching direction is considered important and, accordingly, the procedure necessary to maintain second-order accuracy while performing the linearization is delineated. It is apparent from Eq. (16) that if the pseudotime derivatives are themselves linear, then second-order accuracy requires no more than a simple Crank–Nicolson averaging of the transverse spatial derivatives followed by linearization in the manner of [7]. If the pseudotime derivatives are nonlinear, however, then care is required to maintain second-order accuracy. The problem becomes apparent if, for the moment, attention is devoted to the simple problem of Eq. (10). Here it can easily be shown that even with the simplest of linearizations, i.e., that f^{n+1} is equal to f^n, first-order accuracy in the pseudotime direction is obtained. Thus it is intuitively resonable to expect even a modest linearization (approximation) to f^{n+1} to do better than

first-order accuracy. Turning now to Eq. (16) where pseudotime derivatives contain nonlinearities, it is obvious here that the simplest of linearizations, $H(\phi^{n+1})$ equal to $H(\phi^n)$, completely destroys the solution. Thus considerable care is required in the case of nonlinear pseudotime derivatives. In these circumstances, an advantage is obtained by basing the linearization on an expansion about the $(n + \frac{1}{2})$ level, as outlined below, and this yields

$$\frac{H(\phi^{n+1}) - H(\phi^n)}{\Delta x} = \left(\frac{dH}{d\phi}\frac{\partial\phi}{\partial x}\right)^{n+(1/2)} + O(\Delta x^2); \tag{17}$$

further,

$$\left(\frac{dH}{d\phi}\right)^{n+(1/2)} = \left(\frac{dH}{d\phi}\right)^n + \left(\frac{d^2H}{d\phi^2}\frac{\partial\phi}{\partial x}\right)^n \frac{\Delta x}{2} + O(\Delta x^2) \tag{18}$$

and, of course, in Eq. (17)$(\partial\phi/\partial x)^{n+(1/2)}$ is readily represented by a second-order-accurate finite-difference operator. The critical term in the linearization is then $(\partial\phi/\partial x)^n$ appearing in the expression for $(dH/d\phi)^{n+(1/2)}$, and this term must be represented *without* an $(n + 1)$ level term in the finite-difference operator, otherwise linearity would be lost. However, it is clear that in Eq. (18) a first-order representation of $(\partial\phi/\partial x)^n$ is adequate to preserve overall second-order accuracy and so with a central difference for $(\partial\phi/\partial x)^{n+(1/2)}$ and a backward difference for $(\partial\phi/\partial x)^n$, the result is

$$\frac{H^{n+1}(\phi) - H^n(\phi)}{\Delta x} = \frac{\phi^{n+1} - \phi^n}{\Delta x} \cdot \left[\left(\frac{dH}{d\phi}\right)^n + \left(\frac{d^2H}{d\phi^2}\right)^n \cdot \left(\frac{\phi^n - \phi^{n-1}}{\Delta x_b}\right)\frac{\Delta x}{2}\right] + O(\Delta x^2), \tag{19}$$

[redacted]

Turning now to the specific equations under consideration in the present problem, Eqs. (1) and (2), the foregoing linearizations are readily applied using chain rule differentiation. Considering first the convective term in the marching direction and writing H for $\rho u\tilde{u}$,

$$\frac{H^{n+1} - H^n}{\Delta x} = \left[\frac{\partial H}{\partial \rho}\cdot\frac{\partial \rho}{\partial x} + \frac{\partial H}{\partial u}\cdot\frac{\partial u}{\partial x} + \frac{\partial H}{\partial \tilde{u}}\cdot\frac{\partial \tilde{u}}{\partial x}\right]^{n+(1/2)} + O(\Delta x^2), \tag{20}$$

and expanding each of the derivatives in turn yields

$$\begin{aligned}\left(\frac{\partial H}{\partial \rho}\right)^{n+(1/2)} &= \frac{\partial H^n}{\partial \rho} + \left(\frac{\partial^2 H}{\partial \rho^2}\cdot\frac{\partial \rho}{\partial x} + \frac{\partial^2 H}{\partial u\,\partial \rho}\cdot\frac{\partial u}{\partial x} + \frac{\partial^2 H}{\partial \tilde{u}\,\partial \rho}\cdot\frac{\partial \tilde{u}}{\partial x}\right)^n \cdot \frac{\Delta x}{2} \\ &= (1 + \lambda)(u\tilde{u})^n - \lambda/2(\tilde{u}^n u^{n-1} + u^n \tilde{u}^{n-1}),\end{aligned} \tag{21}$$

where $\lambda = (x_{n+1} - x_n)/(x_n - x_{n-1})$, with similar consequences for $(\partial H/\partial u)^{n+(1/2)}$. Using Eq. (21) in Eq. (20) results in the linear difference operator

$$\frac{\partial}{\partial x}\rho u\tilde{u} = \frac{1}{\Delta x}\left[C_{u\tilde{u}}\rho^{n+1} + C_{\rho\tilde{u}}u^{n+1} + C_{\rho u}\tilde{u}^{n+1} + \tilde{C}\right], \tag{22}$$

where, for example

$$\begin{aligned} C_{\rho u} &= (1+\lambda)(\rho u)^n - \lambda/2(\rho^n u^{n-1} + u^n\rho^{n-1}), \\ -\tilde{C} &= C_{u\tilde{u}}\rho^n + C_{\rho\tilde{u}}u^n + C_{\rho u}\tilde{u}^n, \\ C_u &= (1+\lambda)\,u^n - \lambda/2(u^n + u^{n-1}). \end{aligned} \tag{23}$$

Turning now to a sample convective term not in the marching direction, $\partial(\rho\tilde{u}v)/\partial y$, with centering at the $n + \frac{1}{2}$ level, we have

$$\left(\frac{\partial}{\partial y}\rho\tilde{u}v\right)^{n+(1/2)} = \frac{1}{2}\,\delta_y\{(\rho\tilde{u}v)^{n+1} + (\rho\tilde{u}v)^n\} \tag{24}$$

and

$$\begin{aligned} (\rho\tilde{u}v)^{n+1} &= (\rho\tilde{u}v)^n + \frac{\partial}{\partial\rho}(\rho\tilde{u}v)^n\,(\rho^{n+1} - \rho^n) \\ &\quad + \frac{\partial}{\partial\tilde{u}}(\rho\tilde{u}v)^n\,(\tilde{u}^{n+1} - u^n) + \frac{\partial}{\partial v}(\rho\tilde{u}v)^n\,(v^{n+1} - v) \\ &= (\tilde{u}v)^n\,\rho^{n+1} + (\rho v)^n\,\tilde{u}^{n+1} + (\rho\tilde{u})^n\,v^{n+1} - 2(\rho\tilde{u}v)^n. \end{aligned} \tag{25}$$

It should be noted that the derivation of the linear difference operator for nth-order higher derivatives not in the marching direction follows similarly to that shown above and results only in a change of the order of the spatial difference operator, in the above case δ_y to $\delta_y{}^n$. Since only first-order derivatives appear in the pseudo-time direction, higher derivatives in the marching direction need not be considered. Using the process outlined by Eqs. (22), (23), and (25), the governing equations are linearized and attention is now devoted to the process of solving the resulting coupled linearized system of equations. However, in passing, it should be noted that although in the foregoing attention has been centered on schemes which are second-order accurate in the marching direction, the present linearization is quite general and in combination with say, either a multilevel difference scheme or by the use of iteration, a nonlinear truncation error of any order can be obtained if desired.

Solution of the System of Equations

Application of the linearization to the governing equations, (2) and (3), together with the equation of state, results in a system of equations at each grid point which

in going from pseudotime level n to $n + 1$ may be written in matrix difference operator notation as

$$D_x\Phi^{n+1} = D_y\Phi^{n+1} + D_z\Phi^{n+1} + S, \tag{26}$$

where Φ is the column vector of the dependent variables u, v, ρ and ω. D_x, D_y, and D_z are four-by-four matrices, but contain elements which are in themselves the spatial difference operators. The spatial difference operators associated with the x, y, and z directions are to be found in D_x, D_y, and D_z, respectively. S is a four-row column vector consisting of known quantities. In the present study, to obtain a uniform second-order-accurate scheme, a Crank–Nicolson centering in the marching direction has been performed with centered three-point first and second derivatives in the cross section. The basic scheme, however, is quite general and higher-order differencing both in the cross section and in the marching direction is easily allowed for. Naturally the higher–order schemes would require the variables to be expandable in a Taylor series and introduce more grid points, but this causes little more difficulty than changing from a block-tridiagonal elimination to, for instance, a block-quindiagonal elimination scheme as a result of the higher-order differencing in the cross section. Higher-order differencing in the marching direction simply requires more pseudotime levels to be stored. As mentioned earlier, the linearization scheme easily accommodates the required reduction in nonlinear truncation error. The matrices are given in detail in the Appendix A, and note that for convenience all the Crank–Nicolson type n-level terms have been incorporated into the source term S.

As is well known, the matrix represented by Eq. (26) applied at each grid point requires special treatment in order to obtain the inverse efficiently, and only if the inverse is obtained efficiently can the implicit formulation be competitive with an explicit approach. In the present study, the matrix is inverted to order Δx^2, consistent with the overall scheme truncation error, by means of an approximate but noniterative two-step ADI scheme. The actual scheme used was generated by applying the Douglas–Gunn [10] technique to Eq. (26) and this resulted in the two-step scheme

$$A[(\Phi^* - \Phi^n)/\Delta x] = D_y\Phi^* + D_z\Phi^n + S, \tag{27}$$

$$A[(\Phi^{**} - \Phi^n)/\Delta x] = D_y\Phi^* + D_z\Phi^{**} + S, \tag{28}$$

where, for convenience, the D_x operator has been particularized somewhat. The solution Φ^{**} from the second step of the ADI scheme is accepted as Φ^{n+1}. The computational effort is reduced considerably if in the second step, Eq. (27) is subtracted from Eq. (28), which results in

$$A[(\Phi^{**} - \Phi^*)/\Delta x] = D_z(\Phi^{**} - \Phi^n). \tag{29}$$

Of course, the key feature of ADI methods is the splitting into difference operators D_y and D_z containing all of the differencing appropriate to that particular coordinate direction. Douglas and Gunn were able to show that the ADI scheme given by Eqs. (27) and (28) satisfies the consistency condition under some fairly general assumptions, provided the original difference scheme, Eq. (26), is consistent. They were also able to show unfortunately in less general circumstances, that stability follows from that of the original difference scheme, in this case the two-dimensional analog of the Crank–Nicolson formula. In addition, they showed that the final solution Φ^{**} approximates Φ^{n+1} with an error no worse than Δx^2. Unfortunately, these results, while comforting, provide no guarantees for the equations of fluid mechanics treated here. In view of the complexity of the governing equations only observations based on the actual calculations seem warranted.

To actually solve the two-step scheme specified by Eqs. (27) and (28), Eq. (29) may be written

$$[(A/\Delta x) - D_x]\,\tilde{\Phi} = \tilde{B}, \tag{30}$$

where $\tilde{x} = y, z$ and $\Phi = \Phi^*, \Phi^{**}$, respectively, and $\tilde{B}$ is the appropriate source matrix for this step. When applied at each grid point in the cross section, a system of linear algebraic equations is obtained. Furthermore, the spatial difference operators within the $D_{\tilde{x}}$ matrix when applied to Φ at the ith grid point generate values of $\tilde{\Phi}$ at the $i+1$, i, and $i-1$ grid points, where the i indices are taken in $\tilde{x}$ direction. Thus the product matrix $D_{\tilde{x}}\Phi$ may be decomposed further into three components, such that

$$(D_{\tilde{x}}\tilde{\Phi})_i = D_{\tilde{x}}^{i+1}\tilde{\Phi}_{i+1} + D_{\tilde{x}}{}^{i}\tilde{\Phi}_i + D_{\tilde{x}}^{i-1}\tilde{\Phi}_{i-1} \tag{31}$$

and $D_{\tilde{x}}{}^{k}$, $k = i+1, i, i-1$ is identical to the $D_{\tilde{x}}$ matrix, except that the spatial difference operators in the $D_{\tilde{x}}$ matrix are replaced by the difference weights appropriate to that k-grid point arising from the application of differencing at the i-grid point. The block-tridiagonal structure of each level now becomes apparent if Eq. (30) is rewritten using Eq. (31) so that at each grid point i the result is

$$-D_{\tilde{x}}^{i-1}\tilde{\Phi}_{i-1} + [(A/\Delta x) - D_{\tilde{x}}{}^{i}]\,\tilde{\Phi}_i - D_{\tilde{x}}^{i+1}\tilde{\Phi}_{i+1} = \tilde{B}_i \cdots. \tag{32}$$

As a result, after application of the boundary conditions the system represented by Eq. (32) may be solved by a highly efficient block-tridiagonal elimination scheme, treating the $\tilde{x}$ direction implicitly. The precise scheme used in the present study consisted of applying a Gaussian elimination technique to the tridiagonal matrix (sometimes called the Thomas algorithm) but with the elements of the tridiagonal matrix treated as square submatrices rather than as simple coefficients. The required inverse of the diagonal submatrix was obtained by a Gauss–Jordan reduction.

It should be noted that during the first step of the ADI computation, ω, the cross-sectional velocity in the direction being treated explicitly does not appear at the intermediate level in either the continuity or x-momentum equation. In the y-momentum equation, ω, at the intermediate level, appears only as a result of the stagnation temperature dependence on ω and, consequently, since this stagnation temperature dependence would almost certainly be weak, it seems reasonable to either neglect this dependence or, as is done here, to treat the ω component in the stagnation temperature explicitly. If this approximation is used the z-momentum equation becomes the only equation to contain ω at the intermediate level, and it may be solved by a straightforward application of tridiagonal elimination. The resultant coupled system representing the continuity, x- and y-momentum equations, it thereby reduced from block elements of four-by-four to block elements of three-by-three. A similar situation holds for v, the other cross-sectional velocity, during the second step computation. The resulting saving in computational time is considerable. Subsequently, some check calculations were performed using the coupled four-equation system and the results agreed very well the three coupled and one uncoupled equation systems except near the boundary when a disturbance left the solution domain and the streamwise step was relatively large. In these severe cases the influence of the applied boundary conditions appeared to require the coupled four-equation system for stability and this was done as required.

At this juncture it is worth observing that in general there is a considerable increase in computational effort in solving a block tridiagonal system for say n dependent variables rather than n simple tridiagonal eliminations which would arise if the system were uncoupled. Obviously if the coupling between dependent variables were weak, for instance if the new level u velocity could be satisfactorily computed to the required accuracy by using the old level v, ω, and ρ or some n-level based approximation to the new level, there would be a very considerable gain in efficiency by making this approximation and solving for u in an uncoupled manner. In many simple flows more of this uncoupling could possibly be valid and certainly would result in a saving of computer time. Further uncoupling has not been adopted in the present work as it is an ad hoc approximation and in any event very likely to be invalid in most of the practical applications of interest to the present authors.

Problem Specification and Boundary Conditions

As mentioned earlier, it was desired to evaluate the present procedure on a problem not containing any embedded subsonic (elliptic) region. This precluded, for the time being, flows with solid boundaries and the consequent no-slip boundary condition, although such flows are currently being treated. Instead, a three-dimensional supersonic free-jet exhausting into an ambient supersonic stream was considered. From symmetry considerations only a quadrant of the flow need be

computed, and during the z sweep, first derivatives of u, ω, and ρ with respect to y at the centerline were set to zero using a second-order-accurate one-sided difference formulation. Also, from symmetry v, the velocity in the y direction was set to zero at the centerline. During the y sweep the v and ω boundary conditions are simply interchanged. Note that since at each step of the ADI solution procedure the finite-difference equations represent an approximation to the governing partial differential equations, it is appropriate to apply the physical boundary conditions at the intermediate step.

Outer edge boundary conditions raise some interesting points. As is well known, the system of equations considered in the present paper exhibits a nearly hyperbolic character when the disturbances are weak and the flow Reynolds number high. Thus the boundary of the computational domain can be selected on the outer side of the initial outgoing characteristic (or shock wave) and uniform flow boundary conditions imposed in the undisturbed flow domain. If troublesome, the problem of the growth of the computational domain can be treated by a linear transformation back into a rectangular domain and/or by a nonuniform grid. The special problems which arise (see [11], for instance) in performing accurate calculations when shock waves intersect boundaries, or indeed are present within the solution domain, are not considered in the present study. The principal point of interest now becomes the appearance of dependent variables from outside the solution domain at the implicit level. These variables arise from the use of centered second-order-accurate spatial differentiation and are in no way particular to the implicit formulation. Without any difficulty three of the four external variables can be removed from the equations by imposing the rather weak constraint that the second derivative of any three of the variables with respect to the implicit direction is zero (i.e., implicit linear extrapolation of the external variable). In view of the choice of the computational domain, from a physical point of view this approximation should be a valid one. Consequently, the finite difference representation of the second derivative at the outer edge of the solution domain, when set to zero, provides a physically realistic relationship between the variable outside the domain and the variable at the edge of the domain and one grid point in from the edge. Thus three of the variables outside the domain may be eliminated in favor of the implicit variables within the domain. Since the three momentum equations are second order, the three imposed boundary conditions are not in conflict with the order of the equations. The continuity equation is first order, however, thus permitting only one boundary condition, in this case a previously applied centerline condition. Thus apparently there exists no legal way of applying a boundary condition to eliminate one of the variables outside of the domain. This result arises strictly as a result of the central differencing applied to the first-order continuity equation. In the limit of infinite Reynolds number the problem would also occur with the momentum equations.

There are several ways of dealing with the problem of removing variables from outside the computational domain. First, one-sided differencing could be used as appropriate and the variables outside the domain would no longer appear in the difference formulas. Second, the problem could be overconstrained by application of an extra boundary condition, or third, an "equivalency" condition could be applied wherein at the boundary the order of the governing equation is raised by differentiation to be the same as the order of the difference equation. The resulting discrete form of the differentiated governing equation is then used to eliminate the variable outside of the domain. All three of these techniques were tried in the present problem with varying results.

One-sided differencing at the outer edge. First, special differencing in the region of the boundary seemed very attractive. In the present problem the velocities outside of the domain were eliminated by the application of boundary conditions. The density outside of the domain was then eliminated by utilizing second-order-accurate one-sided derivative formulas for density derivatives in the implicit direction. The resulting scheme behaved poorly. Quite rapidly the solution generated a significant error in the outer edge density and this error propagated rapidly into the solution. Several variants of this scheme were tried, including the use of higher-order one-sided difference formulas, with uniformly poor results. The reason for this behavior was not readily apparent but the one-sided difference approach was not considered satisfactory for use in the present problem. This is, of course, not to say that a change in differencing at the boundary could not be entirely satisfactory in other circumstances. Presumably the apparent unconditional instability with the one-sided difference approximations is explainable within the framework of the stability analysis of Gustafsson, Kreiss, and Sandstrom [12].

Overconstrained solutions. The second approach tried was simply to overconstrain the solution by application of an extra boundary condition. Actually the problem of overconstraint has been studied in some detail with regard to linear first-order hyperbolic systems. Parter [13] considered the error propagation resulting from the application of "wrong" boundary conditions in two explicit schemes. Later, Parter's work was generalized by Kreiss and Lundqvist [14], while subsequently Koster [15] examined the problem of stability arising from the application of extra boundary conditions. Unfortunately, as is often the case in the flow of a real fluid, little direct use can be made of the results obtained from consideration of a first-order linear hyperbolic system. However, it is observed that Parter and Kreiss and Lundqvist noted that the error resulting from the application of the wrong boundary condition would, in their system, propagate inward by an amount proportional to $h \log (h)$, where h is the vertical mesh spacing. It seems reasonable to suppose that the magnitude of the propagated errors would be proportional to the magnitude of the initial error, and Parter showed this to be true in the limit

of zero error, lending support to the thought that in the present problem if a physically acceptable but overconstraining boundary condition were applied and if the overall scheme were stable, the resulting small errors would be restricted to a narrow domain close to the boundary, provided a fine mesh were utilized. Since the outer boundary had been chosen to lie in the undisturbed domain it was physically appropriate to expect the second derivative of density to be zero in this outer flow. Rather than have the solution return the expected value of the second derivative of density, this condition was forced on the system by the application of the extra boundary condition. The resulting scheme appeared quite stable and no significant errors were generated at the boundary, at least until the initial characteristic was allowed to exit from the domain. If permitted, subsequent to the exit of the initial characteristic, the flow would settle down again to be quite uniform in the region of the boundary. Although hardly a definitive test, overconstraining the solution by application of an extra boundary condition, at least for the initial series of calculations, did not appear to result in any significant difficulties.

An equivalency condition. The final approach tried was to eliminate the problem variables by application of an equivalency condition, as opposed to a boundary condition. In the particular instance considered, the source of the problem resides in the fact that the first order continuity equation, when discretized, requires more boundary conditions than the governing equation permits. To circumvent the problem the governing equation is differentiated so that the discrete form of the equations is equivalent, at least insofar as the boundary conditions are concerned. This process need only be carried out at the boundary and the continuity equation differentiated with respect to the implicit direction and the resulting equation used to eliminate the offending variables. This technique, although assuming differentiability, has the attribute that it adds no additional information to the system and, consequently, is not a boundary condition in a true sense but merely an imposed equivalency condition. For simplicity, the initial evaluation of the scheme was carried out on a two-dimensional problem. The appearance of cross derivatives containing both coordinates does present a problem with this scheme for use in multidimensional problems, although it is felt that a lagged evaluation of such cross derivatives suffices. In any case, an evaluation was made by differentiating the continuity equation with respect to the transverse (implicit) direction and this equation was used to eliminate the density outside the domain. The resulting scheme was stable for the range of step sizes investigated and, apparently, quite accurate. As with the overconstrained system, uniform flow of the expected magnitude in the region of the boundary was obtained before and after the outgoing disturbance left the domain. The equivalency scheme, although slightly more laborious, seemed to possess better accuracy capability than the overconstrained solutions, and is described in detail in Appendix B.

In evaluating the results of the initial trials, it was felt that there really was not a great deal of difference between the overconstrained and the equivalency approach. In view of the savings in programming effort, the overconstrained approach was initially utilized throughout. However, it later become clear that when large axial steps were taken, the equivalency technique was much more stable, although with modest axial steps the two procedures behaved similarly. Consequently, the cases with the largest axial steps were, where appropriate, computed using the equivalency technique and this technique is the preferred one at present.

Computational Results

Computed results for a square jet are considered initially; solutions for a rectangular jet will be presented subsequently. The free stream Mach number was fixed at 1.66 and a gas stagnation temperature of 3750° R adopted. The ratio of jet exit centerline velocity to free stream velocity was 1.25 in all cases. A constant velocity core was ascribed to the jet and this core was smoothly faired into the free-stream velocity over a distance of about one-quarter of a jet width using a hyperbolic tangent. A number of cases have been run successfully but only two broad categories are discussed here: first, where the density was specified such that the pressure at the initial plane was constant everywhere; and, second, where the jet pressure was 1.38 times the free stream pressure.

Considering the case of matched initial pressure, calculations were first performed at infinite Reynolds numbers. A Courant–Friedrichs–Lewy (CFL) number (Courant *et al.* [16]) is defined as

$$\Delta x \text{ tanarc sin } M^{-1}/(\Delta y \text{ or } \Delta z),$$

where Δx is the streamwise step, Δy or Δz the cross-sectional step size, and M the streamwise local Mach number. Typically, many conditionally stable methods are evaluated on the basis of what fraction of the unit CFL number they can take for a streamwise step, given some transverse mesh. Indeed, as defined above, a unit CFL number would correspond to the axial step taken by a straightforward method of characteristic procedure integrating from every alternate transverse grid point.

and 48, are shown in Fig. 1; calculations at a CFL number of 24 were not sufficiently different to warrant presentation. In Fig. 1 the profiles of axial velocity at various spanwise locations are shown at an axial location of $x/L_0 = 0.62$, which is about three jet heights downstream. As can be seen from Fig. 1, there was no significant difference between the results at various CFL numbers and, in addition, the exact result that, for a pressure matched situation the inlet profile is convected downstream without alteration was obtained correct to a minimum of five figures

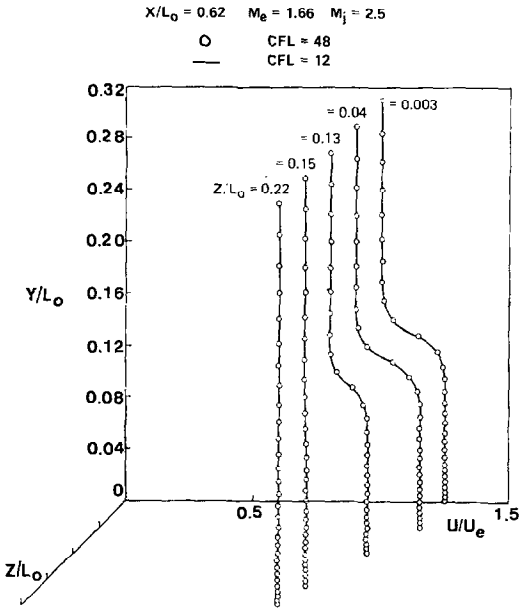

FIG. 1. Rectangular jet velocity profiles at infinite Reynolds number and two CFL conditions.

out of the eight carried by the machine (single precision was used throughout). Some error buildup was noted, however, near the upper boundaries, contaminating the fourth significant figure after twelve jet half-height downstream but this error was quite localized. Calculations were performed by changing from a consistent three-level second-order linearization to a first-order two-level linearization simply by equating the n and $n-1$ levels in the linearized streamwise derivative of $\tilde{u}$ (see Eq. (23)). For the meshes examined, the differences were quite insignificant. Since a quadrant of a square jet was being computed, symmetry of the solution about the diagonal was also checked and at about twelve jet half-heights downstream was held to a minimum of five significant figures on axial velocity except close to the outer boundaries. Computer run times were CFL independent and averaged three minutes of Univac 1110 CPU time to march about eleven streamwise stations with 2025 grid points in the cross section. The circles on Fig. 1 denote the grid points at which the calculations were performed at the selected spanwise locations and, although the calculations were carried out to a y/L_0 of 1, only part of the flow field is shown in Fig. 1.

Considering now the case of low Reynolds numbers, a viscous diffusion number is defined from Eq. (3) by analogy to simple heat flow equation (Richtmyer and Morton [17]) as

$$\Delta x/\mathrm{R_e}\,\rho u(\Delta y \text{ or } \Delta z)^2$$

and for comparative purposes it is observed that in the diffusion dominated case of negligible convection the explicit method derived from a forward difference for the marching direction and centered space difference at the explicit level would be stable for a time step corresponding to a diffusion number less than or equal to $\frac{1}{2}$. Several calculations were performed at low Reynolds numbers with a 45×45 cross-sectional mesh and the results for a jet exit Reynolds number of 11, based on jet half-height, are presented in Fig. 2. A number of different streamwise steps were used and the results at an axial location of $x/L_0 = 0.62$ for axial steps which gave diffusion numbers of 1200 and 300 are shown in Fig. 2. Very little difference in the two solutions can be observed and no difficulties were experienced in performing the calculations. The CFL numbers for these calculations were 48 and 12. The very interesting fluid mechanical observation was made in that although the pressure was constant everywhere at the inlet plane, quite rapidly as the flow developed, pressure gradients formed in the flow. The weak ripple in the axial velocity near the $y/L_0 = 0.14$ location, evident in Fig. 2, was quite pronounced in the pressure profile. The initial velocity profile used for these calculations was, for all practical purposes, identical to that shown in Fig. 1, with the transverse velocities set to zero. After about thirteen jet heights downstream, symmetry was checked and at worst slight discrepancies in the fifth significant figure in axial velocity were obser-

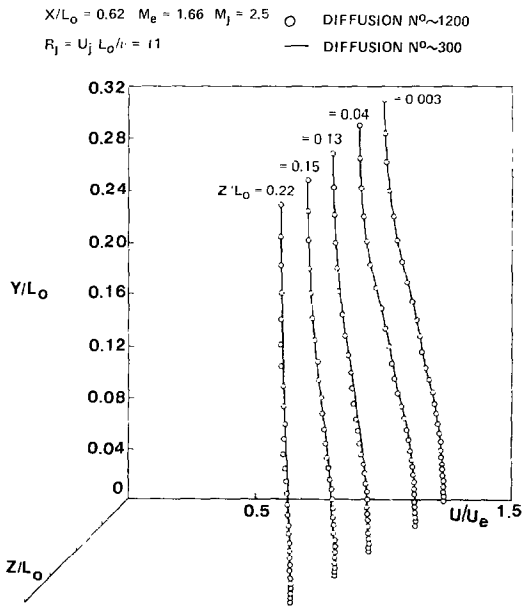

FIG. 2. Rectangular jet velocity profiles at low Reynolds number with various streamwise step sizes.

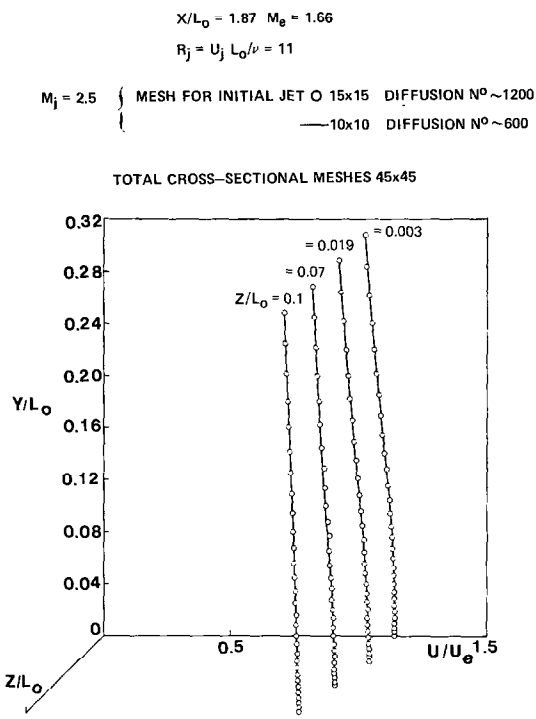

FIG. 3. Rectangular jet velocity profiles at low Reynolds number and two jet cross sectional meshes.

ved. Since diffusion did cause changes at the outer boundaries, it was not clear whether or not significant error buildup at the boundary was occurring.

Also, at a Reynolds number of 11 and a 45 × 45 cross-sectional grid, calculations were performed but in this instance the spatial mesh was locally refined in the jet, with the axial step kept the same. This transverse mesh refinement resulted in a doubling of the diffusion number and profiles of axial velocity approximately nine jet heights downstream are shown in Fig. 3. In this case the circles represent the refined mesh and, as can be seen, the two calculations do not differ significantly. Again, symmetry was checked and at worst slight discrepancies in the fifth figure on axial velocity were observed.

Finally, the inlet density profile was adjusted to provide a jet static pressure of 1.38 times the free-stream static and calculations performed for two Reynolds numbers for a 45 × 45 cross-sectional mesh. Apart from the inlet density profile the inlet conditions were identical to the pressure matched case and the inlet axial velocity profile, as indicated in Fig. 1. The results for a Reynolds number of 11, CFL number of 48, and diffusion number of 1200 are shown in Fig. 4, where

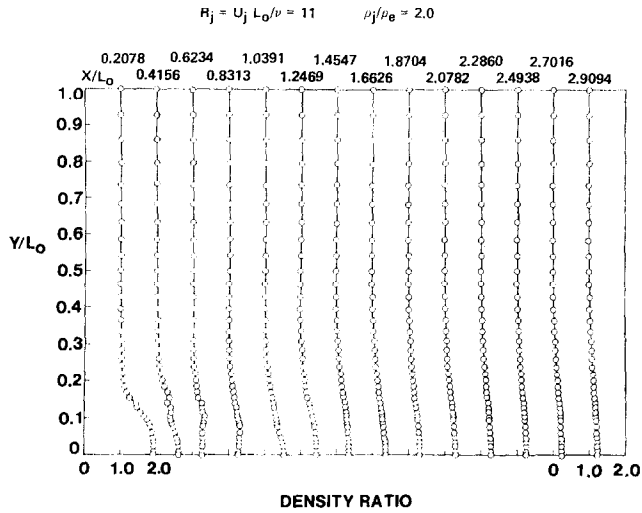

FIG. 4. Underexpanded rectangular jet density profiles at low Reynolds number.

density profiles at various axial locations are shown. Immediately downstream of the inlet plane wiggles develop at the jet free-stream interface but these wiggles are substantially gone by four or five jet heights downstream. Near the jet center the jet initially overexpands, then subsequently compresses. Once again a symmetry check some ten jet heights downstream indicated at worst slight discrepancies in the fifth place on axial velocities. An identical calculation at a Reynolds number of 5×10^3 and CFL number of 50 became unstable after the initial characteristic

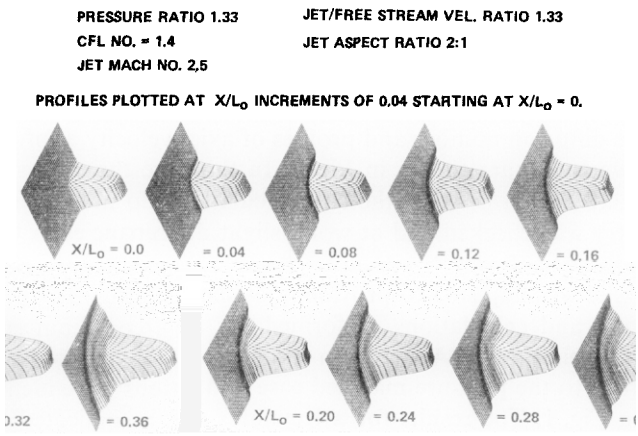

FIG. 5. Underexpanded rectangular jet velocity profiles.

exited from the domain when overconstrained boundary conditions were applied. The calculation was rerun with the equivalency condition applied and a stable solution obtained. From the results it was evident that although stable the axial step was larger than desired in view of the rapid changes in flow properties in the axial direction, particularly near the center of the jet.

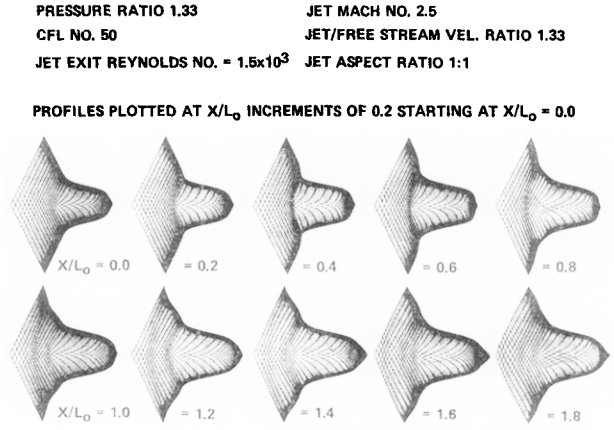

FIG. 6. Underexpanded rectangular jet velocity profiles.

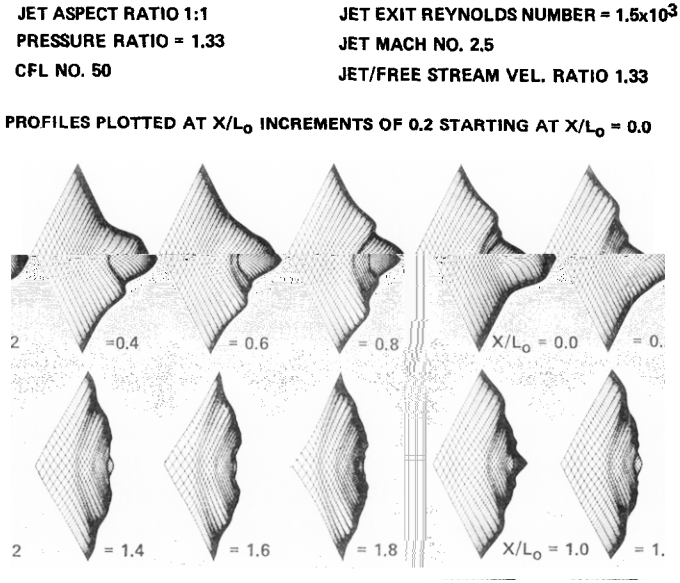

FIG. 7. Underexpanded rectangular jet pressure profiles.

Two additional high Reynolds number cases were run for demonstration purposes. The first of these is for the same overpressured conditions as before and with a jet exit Reynolds number of 5×10^4. However, in this instance a rectangular jet of 2 : 1 aspect ratio was considered. For this particular case a relatively small axial step corresponding to a CFL number of about 1.4 was used with a 40×80 cross-sectional mesh. The velocity profiles at various axial locations downstream of the jet are shown in Fig. 5. The last case presented was again for an overpressured jet and here an attempt was made to better define the flow within the jet itself by refining the mesh in this region. As in the earlier cases, a quadrant of square jet with a 45×45 cross-sectional mesh was used. With the refined mesh and an axial step sufficient to resolve the axial changes, the CFL number corresponding to the axial step was about 50. The severity of the outgoing pressure disturbance required that the calculation be performed using the coupled four-equation system and that the equivalency boundary conditions be imposed. When this was done little difficulty was experienced with the calculation and the velocity profiles are plotted in Fig. 6. In Fig. 7, a plot of the static pressure at various axial locations is given.

Concluding Remarks

There are two potential problem areas commonly associated with implicit methods, neither of which manifested itself in the present study. Both problems arise from the use of central differences and each will be reviewed in turn. Concerning the first problem, Roache [18] has demonstrated that in certain cases with central differences and function boundary conditions the finite-difference solution of a simple convection-diffusion equation possesses an oscillatory solution (i.e., one with "wiggles") when the cell Reynolds number is greater than 2. Now, as a rough guide, in most of the calculations reported in the present note, the cell Reynolds number based on cross-sectional mesh and velocity was approximately 10^{-3} times the Reynolds number based on jet half-height. Calculations were were performed for jet Reynolds numbers of 5×10^3, 5×10^4, and ∞ so that the simple cell Reynolds numbers restriction was violated for a number of test cases without any apparent difficulty. As Roache [18] points out, there are a number of reasons why a multidimensional procedure might not suffer from a cell Reynolds number restriction of less than 2. In a companion study, however, Briley and McDonald [7] did encounter difficulties in a multidimensional problem which were attributed to the violation of a cell Reynolds number limitation. In review, it was concluded that the present procedure did not suffer from the same cell Reynolds number problem for the range of flow conditions investigated because the derivative boundary conditions which were applied did not require rapid variations in the region of the boundary, possibly aided by the low cell Reynolds numbers encoun-

tered near the boundaries and the appearance of a small amount of the diagonal element due to the nonuniform mesh.

The second problem arises at high Reynolds number from the use of central differences on the convective terms. Since central differences with a uniform mesh do not involve the variable at the central mesh point, when large axial steps are taken to exploit the favorable stability properties of implicit methods, the results of this particular set of circumstances is readily seen (for instance, by inspection of Eq. (3)) to reduce the coefficient of the diagonal elements in the momentum equations. Eventually the system of equations ceases to be diagonally dominant and the possibility of significant error arising in the elimination scheme must be acknowledged. It should be noted that loss of diagonal dominance only implies the *possibility* that errors in the elimination scheme may arise, not that they *will* arise. In their study of pure convection in one dimension, Hirsh and Rudy [19] noted that with forward time and centered space differences the resulting system loses diagonal dominance when a time step greater than that corresponding to the usual CFL limit for this equation is taken. However, several points can be made concerning even this simple observation, the first being that with a Crank–Nicolson averaging the loss of diagonal dominance is postponed to twice the aforementioned streamwise step. Second, if attention is devoted to the convective terms in a matching problem of the type studied here, then the form of the linearization used can greatly affect the result. For instance, if nonconservative differencing is used then the cross-sectional velocity scales the spatial difference gradient giving a term $(\rho v)^n u_y$, so that for weak cross flow, loss of diagonal dominance would rarely occur. The conservatively differenced scheme used in the present study was actually quite restrictive in this sense of diagonal dominance. Nonetheless, in the present study, a check of the elimination scheme by back substitution of the solution and computing of residuals revealed no error problem at the highest Reynolds numbers and largest axial steps both for the uniform and nonuniform mesh. Had significant elimination error been detected, consideration would have been given to restructuring the linearization but more than likely, since probably the new linearization would result in a lowering of the order of the nonlinear truncation error, the simple expedient of one-sided differencing on the appropriate convective term would have been adopted. Again, this would be at the expense of lowering the order of the truncation error unless the matrix were expanded to allow more off-diagonal elements. One-sided differencing on the convective term also eliminates any potential cell Reynolds number limitation.

mately half of the computational effort in the type of problem considered here is involved with overhead calculations such as the evaluation of the coefficients of the equations of motion at each grid point. These overhead computations would be fairly independent of the method of integrating the differential equations and,

consequently, even the most efficient of integration schemes would not result in a method more than roughly about a factor of 2 faster per grid point per axial step than the present scheme. However, the demonstrated capability of the present procedure to take a spatial step more in keeping with the rate of change of the solution, rather than be restricted to a step dictated by the computational mesh, is a powerful factor in the methods favor. This is particularly evident in many of the problems facing the present authors, since the stability limitations turn out to be very restrictive and the rate of change of the physical processes permits a large step to be taken if the method is capable of taking it.

Appendix A

The matrix difference operator is given by Eq. (26) and represents the application of the differencing and linearization to the governing equations, in this case Eq. (3). The column vector Φ contains u, v, ρ, and ω in that order and the matrix difference operators are presented in the order of continuity equation; (z, ω) momentum equation; (y, v) momentum equation; and finally, (x, u), the streamwise momentum equation. The A matrix is written

$$
\begin{bmatrix}
C_{\rho} & 0 & C_{u} & 0 \\
C_{\rho\omega} & 0 & C_{u\omega} & C_{\rho u} \\
C_{\rho v} & C_{\rho u} & C_{uv} & 0 \\
2(1+B)C_{\rho u} & 2BC_{\rho v} & (1+B)C_{uu} + A + BC_{vv} + BC_{\omega\omega} & 2BC_{\rho\omega}
\end{bmatrix}
$$

Turning now to the D matrices, the notation is adopted that a spatial difference operator δ occurring outside a curly parenthesis indicates that the matrix multiplicative variable is to be inserted within the parenthesis prior to differencing. With this convention the D_y matrix is written

$$
-\frac{1}{2}\left[\begin{array}{c|c|c|c}
0 & \delta_y\{\rho^n\cdot\} & \delta_y\{v^n\cdot\} & 0 \\
\hline
0 & \delta_y\{(\rho\omega)^n\cdot\} & \delta_y\{(v\omega)^n\cdot\} & \begin{array}{c}\delta_y\{(\rho v)^n\cdot\} \\ -R_e^{-1}\,\delta_y^2\{\ \}\end{array} \\
\hline
B\delta_y\{2(\rho u)^n\cdot\} & \begin{array}{c}(1+B)\delta_y\{2(\rho v)^n\cdot\} \\ -R_e^{-1}\,\delta_y^2\{\ \}\end{array} & \begin{array}{l}\delta_y\{(v^2)^n\cdot\}+ \\ A\,\delta_y\{\ \}+B\delta_y\{[u^2 \\ +v^2+\omega^2]^n\cdot\}\end{array} & B\,\delta_y\{2(\rho\omega)^n\cdot\} \\
\hline
\begin{array}{c}\delta_y\{(\rho v)^n\cdot\} \\ -R_e^{-1}\,\delta y^2\{\ \}\end{array} & \delta_y\{(\rho u)^n\cdot\} & \delta_y\{(uv)^n\cdot\} & 0
\end{array}\right]
$$

As indicated in the text, the D_x matrix is in fact the composite of n identical constituent matrices, $D_x{}^n$, where n is the number of grid points used in the difference operators δ_x and $\delta_x{}^2$, with the sole distinction that each of the n constituent matrices has the difference operator replaced by the weight appropriate to that grid point Following the same convection, the D_z matrix is written

$$
-\frac{1}{2}\left[\begin{array}{c|c|c|c}
0 & 0 & \delta_{\pm}\{\omega^n\cdot\} & \delta_{\pm}\{\rho^n\cdot\} \\
\hline
B\delta_{\pm}\{2(\rho u)^n\cdot\} & B\delta_{\pm}\{2(\rho v)^n\cdot\} & \begin{array}{l}\delta_{\pm}\{(\omega^2)^n\cdot\}+A\delta_{\pm}\{\ \} \\ +B\,\delta_{\pm}\{[u^2 \\ +v^2+\omega^2]^n\cdot\}\end{array} & \begin{array}{c}(1+B)\,\delta_{\pm}\{2(\rho\omega)^n\cdot\} \\ -R_e^{-1}\,\delta_{\pm}^2\{\ \}\end{array} \\
\hline
0 & \begin{array}{c}\delta_{\pm}\{(\rho\omega)^n\cdot\} \\ -R_e^{-1}\,\delta_{\pm}^2\{\ \}\end{array} & \delta_{\pm}\{(v\omega)^n\cdot\} & \delta_{\pm}\{(\rho v)^n\cdot\} \\
\hline
\begin{array}{c}\delta_{\pm}\{(\rho\omega)^n\cdot\} \\ -R_e^{-1}\,\delta_{\pm}^2\{\ \}\end{array} & 0 & \delta_{\pm}\{(u\omega)^n\cdot\} & \delta_{\pm}\{(\rho u)^n\cdot\}
\end{array}\right]
$$

and, finally, the S matrix is written

$$
-\frac{1}{2}\begin{bmatrix}
0 \\
-\delta_y(\rho v\omega)^n - \delta_x(\rho\omega^2)^n - R_e^{-1}\left[\delta_y^2(\omega^n) + \delta_x^2(\omega^n)\right] \\
+A\delta_x(\rho^n) - B\delta_x\left\{\rho u^2 + \rho v^2 + \rho\omega^2\right\}^n \\
-\delta_y(\rho v^2)^n - \delta_x(\rho v\omega)^n - R_e^{-1}\left[\delta_y^2(v^n) + \delta_x^2(v^n)\right] \\
+A\delta_y(\rho^n) - B\delta_y\left\{(\rho u^2) + (\rho v^2) + (\rho\omega^2)\right\}^n \\
-\delta_y(\rho uv)^n - \delta_x(\rho u\omega)^n - R_e^{-1}\left[\delta_y^2(u^n) + \delta_x^2(u^n)\right]
\end{bmatrix}
$$

Appendix B

Considering the first ADI sweep to be implicit in the y direction and the second sweep to be implicit in the z direction, the continuity equation, Eq. (2), is differentiated with respect to y and z and then split into the ADI format. For the z-differentiated equation the split-differenced from of the equation is written as the difference between the ** and the * level variables; that is, between the $n+1$ and the intermediate level variable. With the linearization and Crank–Nicolson averaging performed the y-differentiated continuity equation may be written

$$(2/\Delta x)\,\delta_y(u^n\rho^* + \rho^n u^* - 2\rho^n u^n) + \delta^2{}_y(\rho^n v^* + v^n\rho^*) + 2\delta_z\delta_y(\rho^n\omega^n) = 0$$

and the z-differentiated equation written

$$(2/\Delta x)\,\delta_z(\rho^n u^{**} + u^n\rho^{**} - \rho^n u^* - u^n\rho^*) + \delta_z{}^2(\rho^n\omega^{**} + \omega^n\rho^{**} - 2\rho^n\omega^n) = 0.$$

When either of the above equations is applied at or adjacent to the boundary it provides a relationship between the variables outside the solution domain and the variables within the domain. With three-point one-sided formulas for the difference operators applied at the point immediately outside the solution domain and the

introduction of all the other boundary conditions, the relationship may be written in matrix notation as

$$Iz_{i+1} = Ez_i + Fz_{i-1} + H,$$

where E, F, and I are four-by-four square matrices and H is a column vector comprised of four rows. The differential continuity equation can be applied at the actual boundary of the solution domain and central differences used to represent the derivatives. Such an application of the technique can eventually give rise to problems in severe cases when the coefficient of the central point is very small. This problem is eliminated by applying the differentiated equation at the point adjacent to but outside the solution domain and using one-sided differences. With three grid points the one-sided second derivatives are first order, but for small v and ω carry little weight in the equation, particularly since the additional boundary conditions are that certain second derivatives are zero. High-order one-sided formulas can be incorporated and the appearance of Z_{I-2} in the matrix may be treated by a straightforward but special elimination. Higher-order difference schemes were in fact evaluated in the uncoupled system but it was felt that little was to be gained in utilizing such a scheme in the coupled system, for the moment. As was mentioned earlier, the additional boundary condition used throughout was that at the outer boundary the second derivative with respect to the implicit direction of u, v, and ω be zero. Such boundary conditions are essentially uncoupled in that they give rise to an equation containing only one of the four dependent variables. The boundary conditions were ordered so that the resulting one nonzero element lay on the diagonal of the E, F, H, and I matrices. More general coupled boundary conditions such as arise from the differentiated continuity equation give rise to an equation containing more than one of the dependent variables so that the row representing the coupled boundary condition contain off-diagonal elements in the E, F, H, I matrices. It is evident that there is no particular difficulty in allowing additional coupled boundary conditions at either the inner or outer edge of the domain in lieu of the uncoupled conditions suggested previously.

In the overall block tridiagonal elimination process the variables outside the solution domain, designated by the subscript $NE + 1$, may be eliminated by the replacement

$$Z_{NE+1} = I^{-1}EZ_{NE} + I^{-1}FZ_{NE-1} + I^{-1}H,$$

where I^{-1} is the inverse of the I matrix. The above derivation is carried out for the fully coupled system of governing equations. The extension for the case where one of the governing equations is solved independently is obtained by removing the appropriate row from the E, F, H, and I matrices. The implication is, of course, that not only must the governing equation itself be essentially uncoupled but so also must be the boundary conditions imposed upon the uncoupled equation.

ACKNOWLEDGMENT

The authors are indebted to Mr. B. Anderson of NASA Lewis Research Center for kindly constructing the plots presented in Figs. 5–7.

REFERENCES

1. L. S. CARETTO, R. M. CURR, AND D. B. SPALDING, *Comput. Meth. Engrg.* **1** (1973), 39–51.
2. S. V. PATANKAR AND D. B. SPALDING, *Internat. J. Heat Mass Transfer* **15** (1972), 1787–1806.
3. W. R. BRILEY, *J. Computational Phys.* **14** (1974), 8–28.
4. C. T. NARDO AND R. J. CRESCI, *J. Computational Phys.* **8** (1971), 268–284.
5. S. G. RUBIN AND T. C. LIN, *J. Computational Phys.* **9** (1972), 339–364.
6. W. R. BRILEY AND H. MCDONALD, Computation of Three-Dimensional Turbulent Subsonic Flow in Curved Passages, United Aircraft Research Laboratories Report R75-911596-8, March 1975.
7. W. R. BRILEY AND H. MCDONALD, Solution of the Three-Dimensional Compressible Navier–Stokes Equations by an Implicit Technique, in "Proceedings of the Fourth International Conference on Numerical Methods in Fluid Dynamics," Springer–Verlag, New York, 1975. See also United Aircraft Research Laboratories Report M911363-6, November 1973.
8. W. F. AMES, "Numerical Methods for Partial Differential Equations," Barnes & Noble, New York, 1969.
9. D. U. VON ROSENBERG, "Methods for the Numerical Solution of Partial Differential Equations," American Elsevier, New York, 1969.
10. J. DOUGLAS AND J. E. GUNN, *Numer. Math.* **6** (1964).
11. N. A. MESSINA AND S. I. CHENG, A Study of the Computation of Regular Shock Reflection With Navier–Stokes Equations, Princeton University, Department of Aeronautics and Mechanical Sciences Internal Memo No. 43, 1973.
12. B. GUSTAFSSON, H. O. KREISS, AND A. SUNDSTROM, *Math. Comp.* **26** (1972), 649–686.
13. S. V. PARTER, *Numer. Math.* **14** (1962), 277–292.
14. H. O. KREISS AND E. LUNDQVIST, *Math. Comp.* **22** (1968), 1–12.
15. D. E. KOSTER, *SIAM J. Numer. Anal.* **10** (1973), 1039–1046.
16. R. COURANT, K. FRIEDRICHS, AND H. LEWY, *IBM Systems J.* (March 1967), pp. 215–234. Also, *Math. Ann.* **100** (1928), 32–74.
17. R. D. RICHTMYER AND K. W. MORTON, Interscience Tracts in Pure and Applied Mathematics, Vol. 4, 2nd Ed., Interscience, New York, 1967.
18. P. J. ROACHE, "Computational Fluid Dynamics," Hermosa, Albuquerque, N. Mex., 1972.
19. R. S. HIRSH AND D. H. RUDY, *J. Computational Phys.* **16** (1974), 304–310.